On the reconstruction of the coronal magnetic field from coronal Hanle / Zeeman observations

M. Kramar & B. Inhester

Max-Planck Institute for Solar System Research

GERMANY

Lindau 2005

Coronal Magnetic Field

Magnetic field contains the dominant energy per unit volume in the solar corona

State-of-the-art determination of the coronal magnetic field:

- Extrapolation of photospheric magnetic sources
- MHD simulations.

Disadvantage: These methods are very ill-posed,

small errors in measurements cause big uncertainty in the corona.

Difficulties of direct measurements at optical wavelengths:

- Coronal plasma is extremely hot (~10^6 K)
- Magnetic fields in the quiet-Sun corona are weak (~10G)

→ line broadening bigger than Zeeman splitting

Alternative: Direct Zeeman-effect measurements in IR range (*Lin et al. 2004*)

Can this data be used for reconstruction of the coronal magnetic field?

Measurements of magnetic field effects in the corona are difficult but possible

- Faraday - effect

  Rotation of polarization plane of polarized light coming from radio-sources and passing through the corona

- Resonance scattering (Hanle – effect)

  Degree and orientation of linear polarization of light scattered by coronal FeXIII and FeXIV ions.

- Longitudinal Zeeman - effect

  Line splitting of circular polarized infrared light scattered by coronal FeXIII ions.

Coronal emission

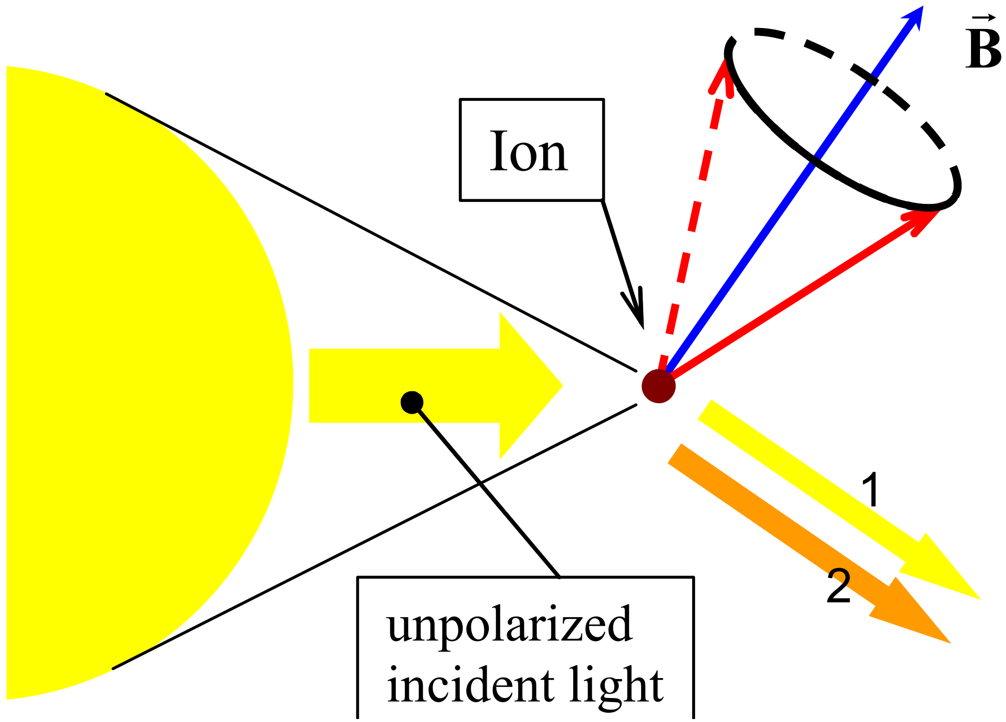

Effects for determination the coronal magnetic field:

- **Hanle effect** contains information only about orientation of the ***B***

- **Zeeman effect** gives the projection of the ***B*** on the LOS

Both are integrated along the line-of-sight (LOS)

Excitation mechanisms:
1) by anisotropic unpolarized radiation from photosphere
2) thermal excitation

Longitudinal Zeeman-effect in the Corona

- High temperature (10^6 K)

Thermal broadening	$\Delta\lambda_D \sim \lambda$
Zeeman splitting	$\Delta\lambda_B \sim \lambda^2$

$\Rightarrow$

Infrared wavelength are more favorable:
λ=10747 Å of Fe XIII

- Weak field (~10 G)

Magnetograph formula (Casini & Judge 1999):

$$\varepsilon_V(\omega,\vec{\Omega}) = k \cdot \bar{g} \cdot \frac{d\varepsilon_I(\omega,\vec{\Omega})}{d\omega} \cdot \frac{e}{2m_e} \cdot B \cdot \cos\theta,$$

$$k = \frac{1 + a \cdot \sigma}{1 + b \cdot \sigma \cdot \left(3\cos^2\theta - 1\right) \cdot 2^{-3/2}}$$

$$\theta = LOS \,\hat{,}\, \vec{B}$$

ε_I and ε_V are emission coefficients for the Stokes I and V components,

$\bar{g}$ is effective Lande factor,

σ is alignment factor, $\sigma(\Theta, R, T, N)$, where $\Theta = \vec{R} \,\hat{,}\, \vec{B}$

for the 10747 A line of the Fe XIII $\sigma < 0.7$

Longitudinal Zeeman-effect in the Corona: Observations

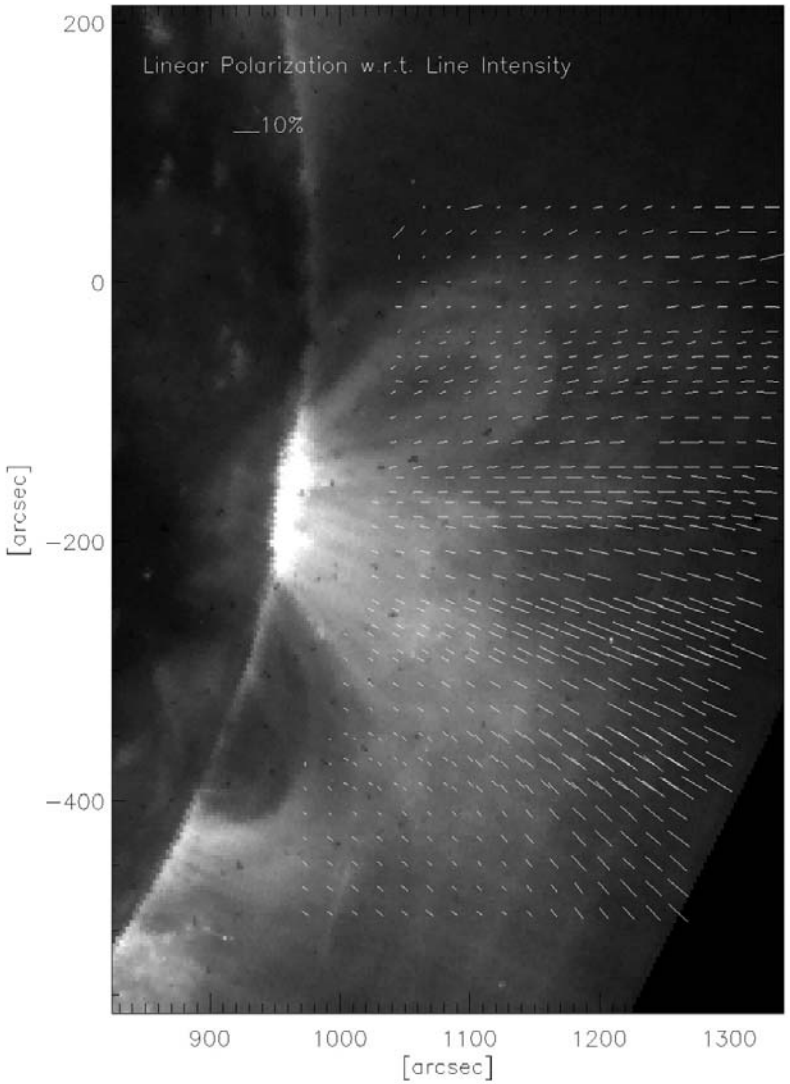

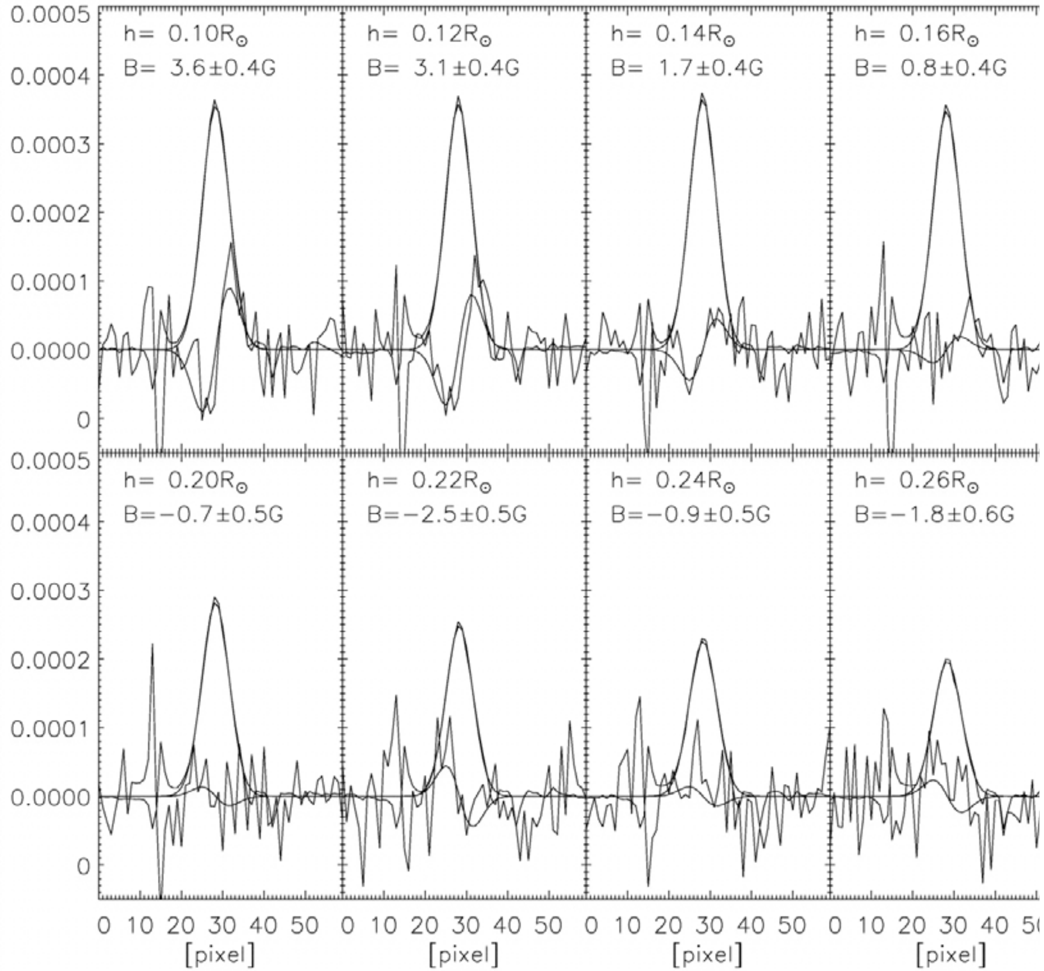

Lin et al. 2004

Zeeman-effect: Magnetograph formula

$$\varepsilon_V(\omega,\vec{\Omega}) = \bar{g} \cdot \frac{d\varepsilon_I(\omega,\vec{\Omega})}{d\omega} \cdot \frac{e}{2m_e} \cdot B \cdot \cos\theta, \qquad \theta = \widehat{LOS, \vec{B}}$$

$$V = \int\limits_{LOS} \varepsilon_V \, dl = \bar{g} \frac{e}{2m_e} \int\limits_{LOS} \frac{d\varepsilon_I(\omega,\vec{\Omega})}{d\omega} \cdot B \cdot \cos\theta dl$$

population density of the exited level

Voigt-function

$$\varepsilon_I(\omega,\vec{\Omega}) = N_{ex.level} \frac{\hbar\omega}{4\pi} \Phi(\omega) \cdot \left[1 + b\sigma \cdot (3\cos^2\theta - 1)\right]$$

σ is alignment factor, $\sigma(\Theta, R, T, N_e)$ (*Casini & Judge 1999*)

if $\sigma << 1$, $\varepsilon_I(\omega,\vec{\Omega}) \to \varepsilon_I(\omega)$ (no directional dependence).

$$\Downarrow$$

$$\frac{dI(\omega)}{d\omega} = \int\limits_{LOS} \frac{d\varepsilon_I(\omega)}{d\omega} dl \Rightarrow$$

from observations

$\dfrac{d\varepsilon_I(\omega)}{d\omega}$ can be found by scalar field tomography

we do not need to know distribution
of the ion density and temperature over corona

Hanle – effect

- Resonance scattering for lines, with lifetime >> Larmor period

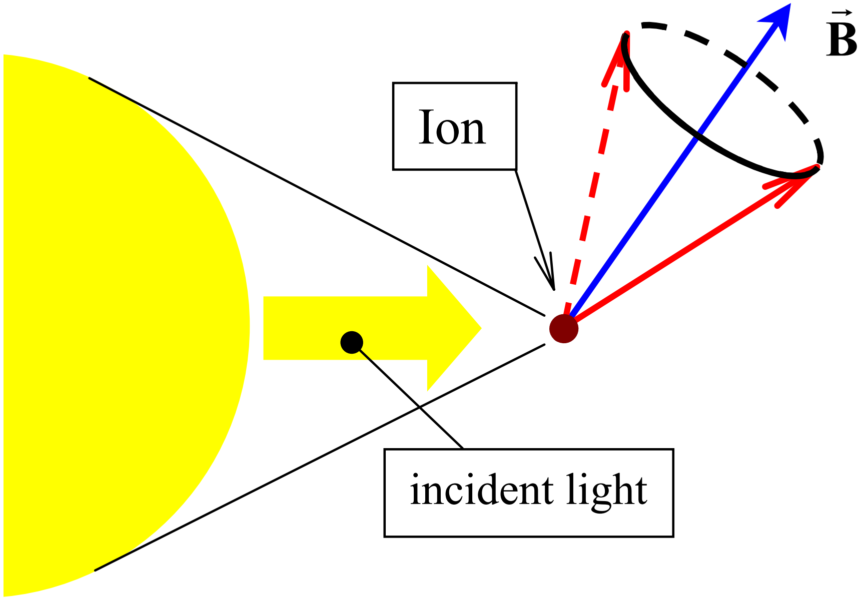

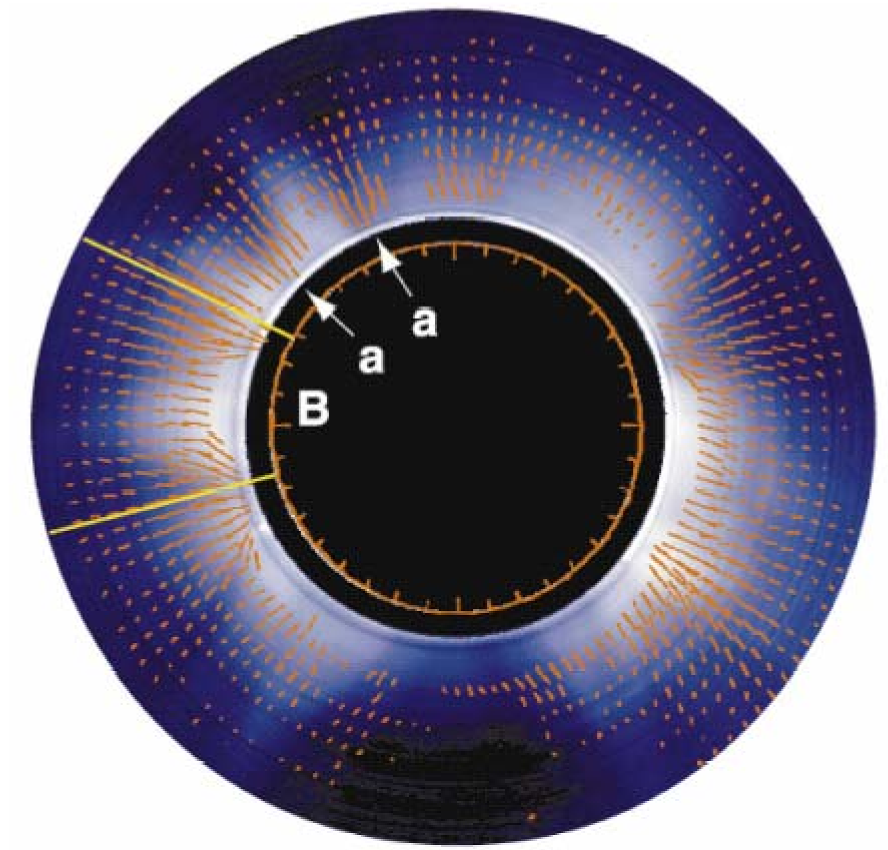

Polarized intensity map of the FeXIII line emission
(Habbal S.R. et al, ApJ **558**, 2001)

Hanle – effect (FeXIII & FeXIV)

$$\frac{\partial \mathbf{S}(\nu,\vec{\Omega})}{\partial l} = -\mathbf{K}(\nu,\vec{\Omega})\cdot\mathbf{S}(\nu,\vec{\Omega}) + \mathbf{E}(\nu,\vec{\Omega}),$$

$$\mathbf{S} = \begin{pmatrix} I & Q & U & V \end{pmatrix}^{\mathrm{T}}, \quad \mathbf{E} = \begin{pmatrix} \varepsilon_I & \varepsilon_Q & \varepsilon_U & \varepsilon_V \end{pmatrix}^{\mathrm{T}} = \begin{pmatrix} \varepsilon_0 & \varepsilon_1 & \varepsilon_2 & \varepsilon_3 \end{pmatrix}^{\mathrm{T}}$$

$$\varepsilon_i(\nu,\vec{\Omega}) = \frac{h\nu}{4\pi} N \sum_{\alpha_l J_l} \sum_{\alpha_u J_u} (2J_u + 1)\cdot A_{\alpha_u J_u \to \alpha_l J_l} \times$$

$$\times \sum_{M_u M_u' M_l q q'} 3 \begin{pmatrix} J_u & J_l & 1 \\ -M_u & M_l & -q \end{pmatrix} \begin{pmatrix} J_u & J_l & 1 \\ -M_u' & M_l & -q' \end{pmatrix} \times$$

$$\times \mathrm{Re}\left[T_{qq'}(i,\vec{\Omega}) \cdot \rho_{\alpha_u J_u}(M_u', M_u) \cdot \Phi(\nu, T, B, v_A) \right]$$

Spherical Tensor (includes viewing geometry and orientation of magnetic field vector)

Density Matrix element

Voigt-function

B ~ 10 G
$A = 1/\tau = 14\ \mathrm{s}^{-1}$ for Fe XIII
$A = 1/\tau = 60\ \mathrm{s}^{-1}$ for Fe XIV

$\int \varepsilon_i(\nu,\vec{\Omega})\,d\nu$ does not depend on the strength of the magnetic field for FeXIII and FeXIV

Hanle – effect

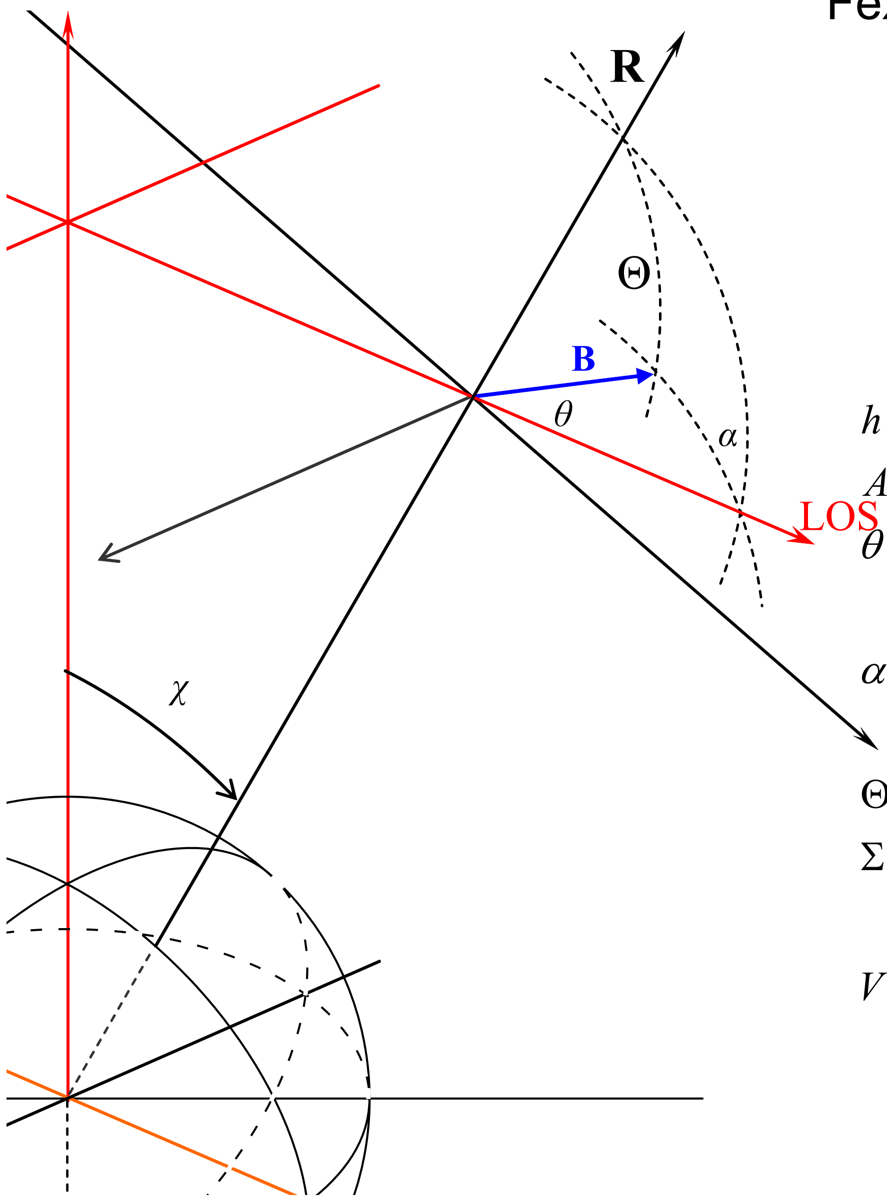

FeXIII and FeXIV ions (Querfeld 1982)

$$\begin{bmatrix}\varepsilon_I\\ \varepsilon_Q\\ \varepsilon_U\\ \varepsilon_V\end{bmatrix}=\frac{3h\nu A}{8\pi}\begin{bmatrix}4\Sigma+\Delta\left(3\cos^2\theta-1\right)\left(3\cos^2\Theta-1\right)\\ \Delta\cdot\left(3\cos^2\Theta-1\right)\cdot\sin^2\theta\cos 2\alpha\\ \Delta\cdot\left(3\cos^2\Theta-1\right)\cdot\sin^2\theta\sin 2\alpha\\ 0\end{bmatrix}$$

$h\nu$ is photon energy;

A is the Einstein coeff. for spontaneous emission;

θ is the angle between the magnetic field direction and the LOS to the observer;

α is the angle between the local radius and the observed polarization projected on the POS;

Θ is the angle between local radius and magnetic field direction

Σ and Δ are proportional to the Zeeman sublevel populations (depends on the properties of incident light, T, N);

$V(\Theta)=3\cos^2\Theta-1$ is the van Vleck factor

There is no information about magnetic field strength!

Hanle – effect (FeXIII & FeXIV)

Orientation of the polarization planes

Dipole Field Quadropole Field

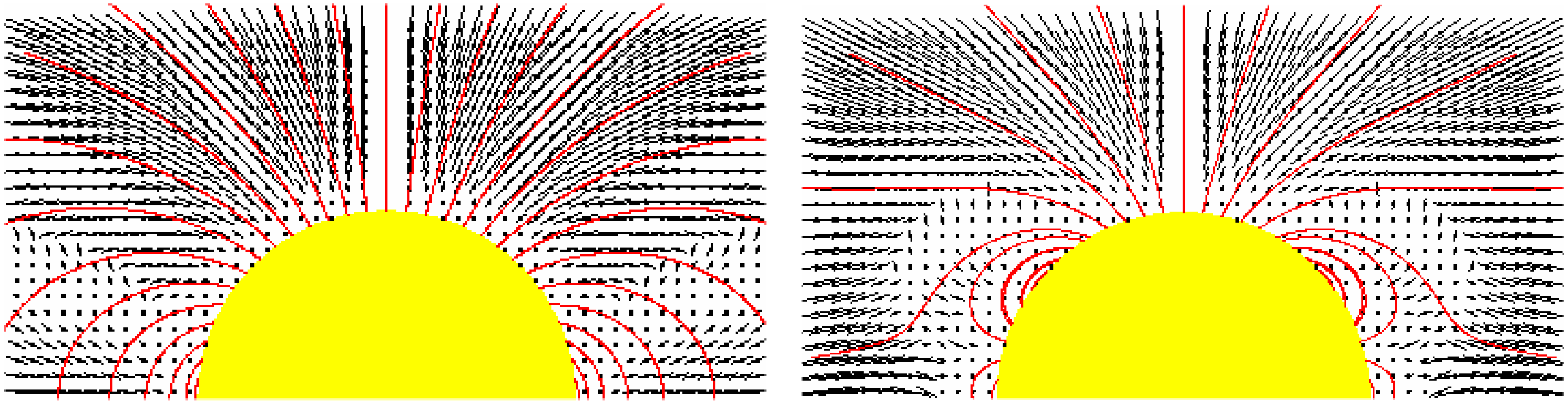

Electron density $N_e \sim r^{-5}$ (Newkirk et al. 1970)
The length of the lines is proportional to degree of polarization.
Red lines are magnetic field lines in the POS.
Orientation of the polarization plane in respect to the magnetic field lines depends on the van Vlek factor $(3\cos^2\Theta - 1)$,
where Θ is angle between **B** and **r**

Scalar Field Tomography

Is This the Kind of Data Which Can Be Used in the Vector Tomography to Reconstruct **B**?

Zeeman data for example

$$D(t,\theta) = \int f(\vec{r}) \cdot B_{\parallel} dl$$

$f(\vec{r})$ can be found by scalar - field tomography

Assumption: alignment factor $\sigma \rightarrow 0$.

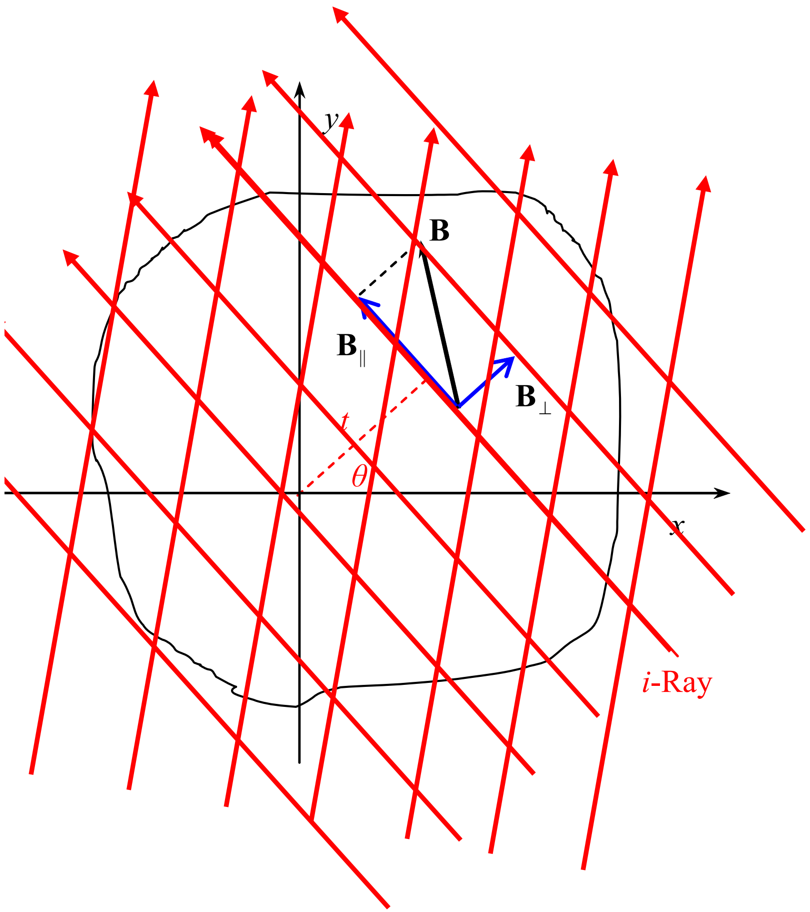

Contrary to scalar-field tomography,
the integrand now depends on the view direction.

For 3-D case we have 3 times more variables to be found than for scalar field but the same number of equations

=> Reconstruction is underdetermined

A General Problem with Vector Tomography

Depending on the observation only the divergence-free or source-free field component can be reconstructed.
For example, for Zeeman-effect data:

$\vec{\mathbf{B}} = \nabla \cdot \Phi + \nabla \times \vec{\mathbf{\Psi}}$ measurements of $\int B_{\|} ds$

$\nabla \cdot \Phi$ *Irrotational component cannot be reconstructed*

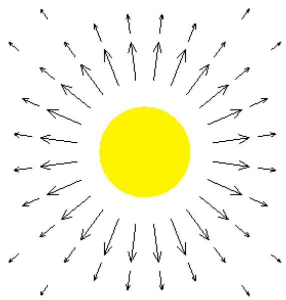

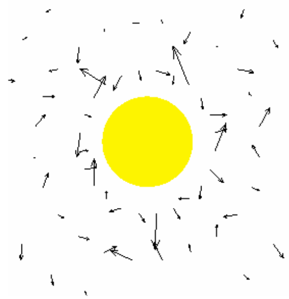

Original Field *Reconstruction*

$\nabla \times \vec{\mathbf{\Psi}}$ *Solenoidal component can be uniquely reconstructed*

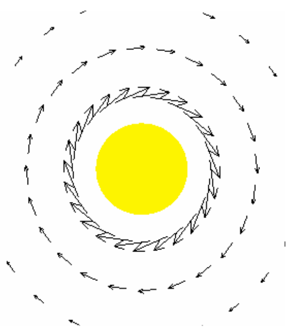

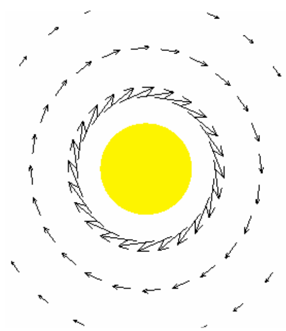

Vector Field Tomography: Regularization

We need additional information about field:

Magnetic field is divergence-free: $\nabla \cdot \vec{\mathbf{B}} = 0$

$$F = \sum_{i=1}^{\text{Number of Rays}} \left(D_i^{\text{sim}} - D_i^{\text{obs}}\right)^2 \quad + \quad \mu \cdot \int_{Corona} \left|\nabla \cdot \vec{\mathbf{B}}\right|^2 dV$$

Should be minimized

Nice properties of this regularization:

- makes the use of photospheric ***B*** observation as boundary condition
- reproduces standard potential ***B*** if *div*-term alone is minimized

Vector Field Tomography: Regularization

- Problem is badly conditioned, e.g.
  number of unknown variables exceeds the number of equations
- Random noise in the data

In result, there is possible no unique reconstruction. Problem is ill-conditioned.

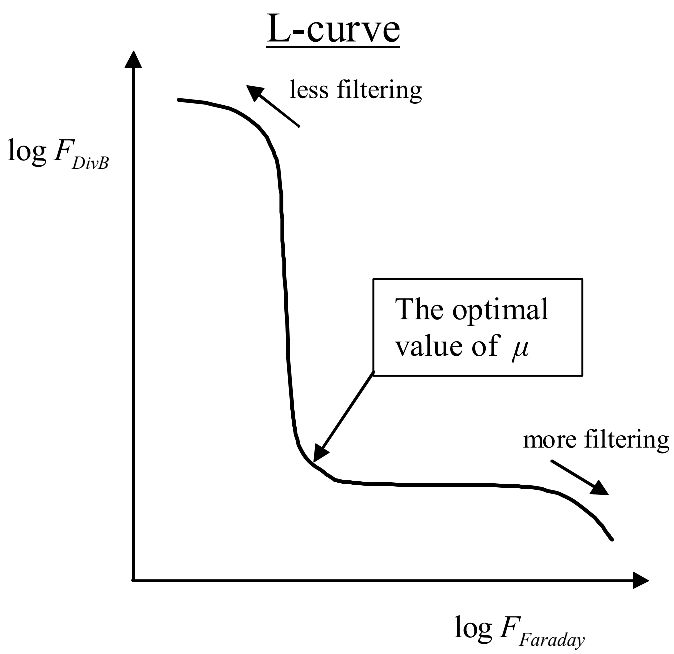

$$F = \sum_{i=1}^{\text{Number of Rays}} \left(D_i^{\text{sim}} - D_i^{\text{obs}}\right)^2 + \mu \int_{Corona} \left|\nabla \cdot \vec{\mathbf{B}}\right|^2 dV =$$

$$= F_{tomo} + \mu \cdot F_{DivB}$$

Tikhonov regularization maximises the smoothness of the solution.

The optimal μ is where the L-curve has its strongest positive curvature

Model Field Configuration for the Tests

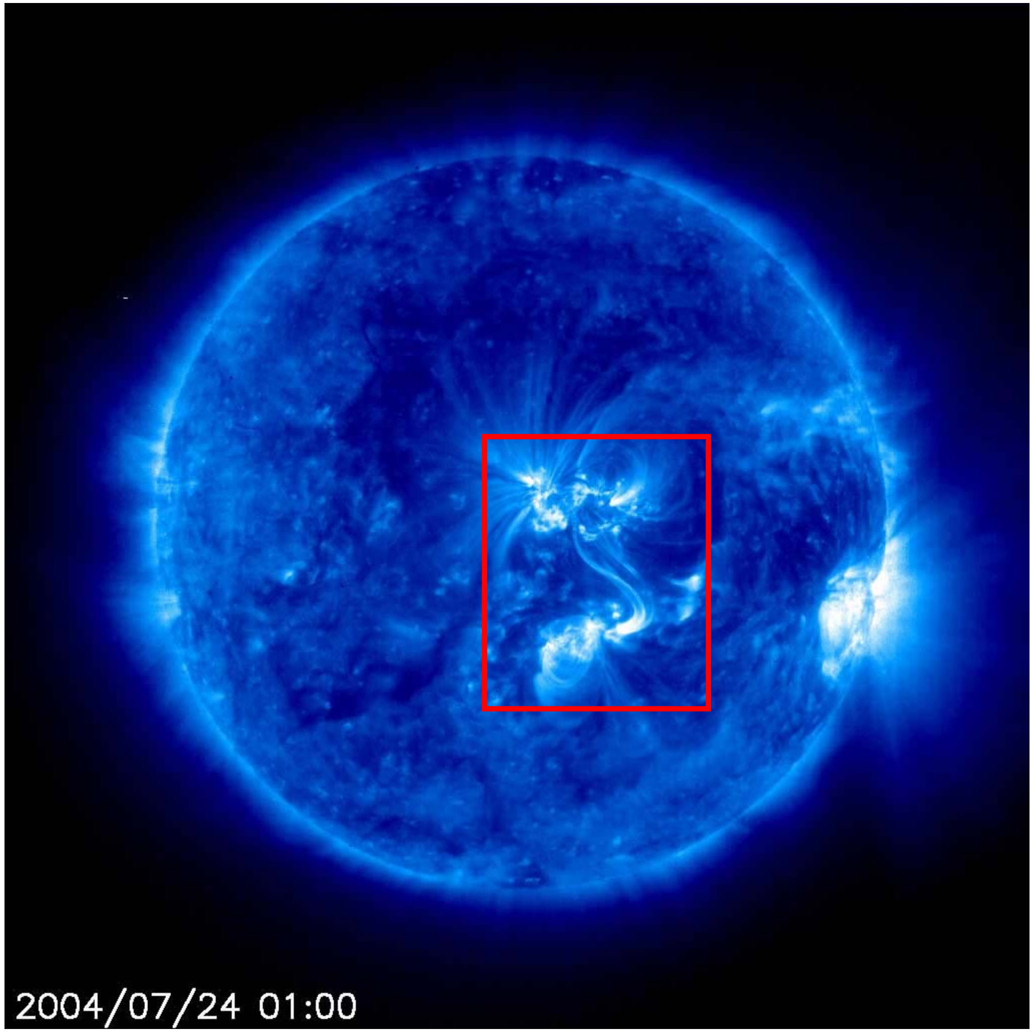

EIT Observation

Dipole + current loop

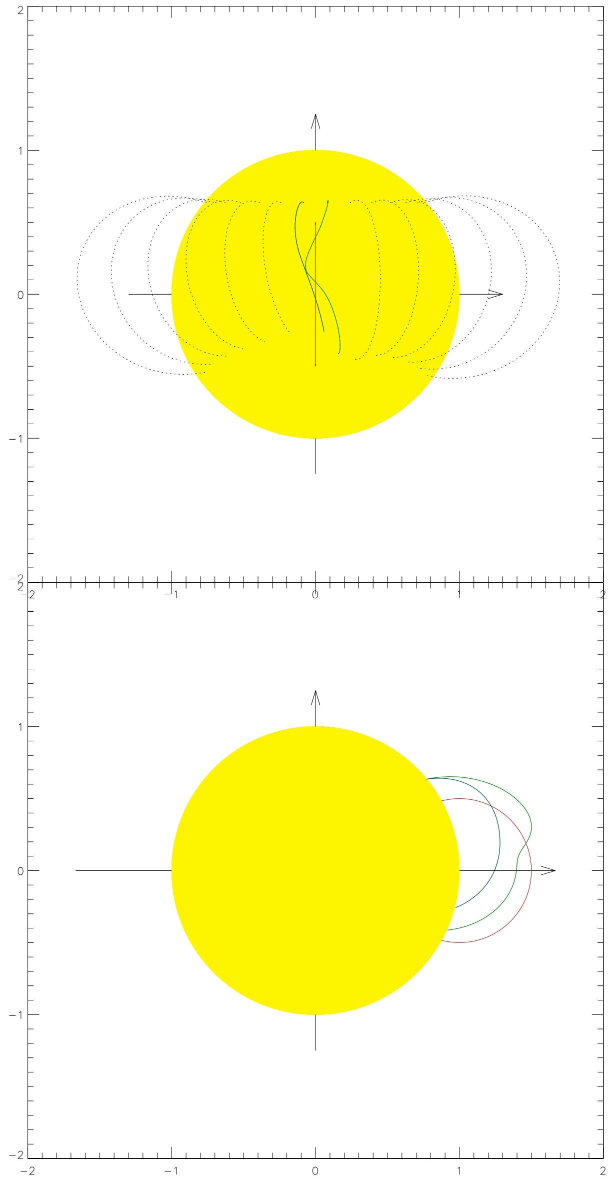

Vector Field Tomography:
2D Example for Zeeman-effect

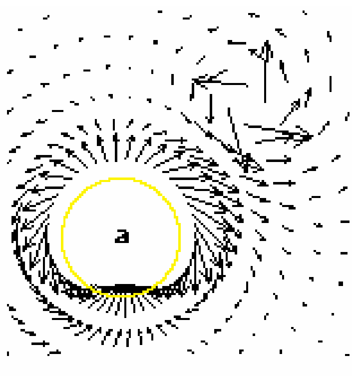

Original Field

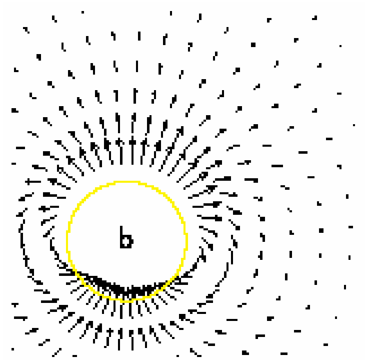

Reconstruction ignoring any tomography data and minimizing F_{divB}-term alone.

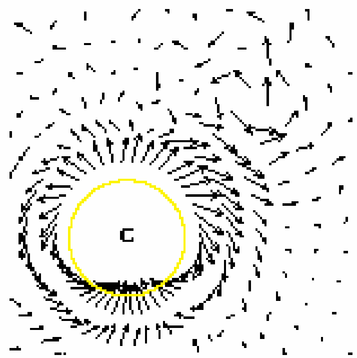

Result of a reconstruction using a random 9% selection of a complete tomography data set.

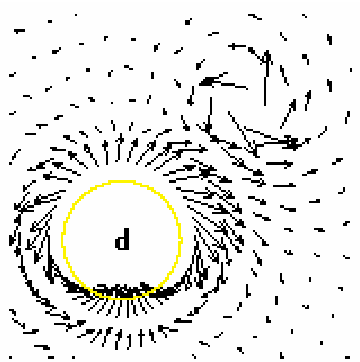

Result of a reconstruction using a random 48% selection of a complete tomography data set.

Reconstruction for Zeeman-effect

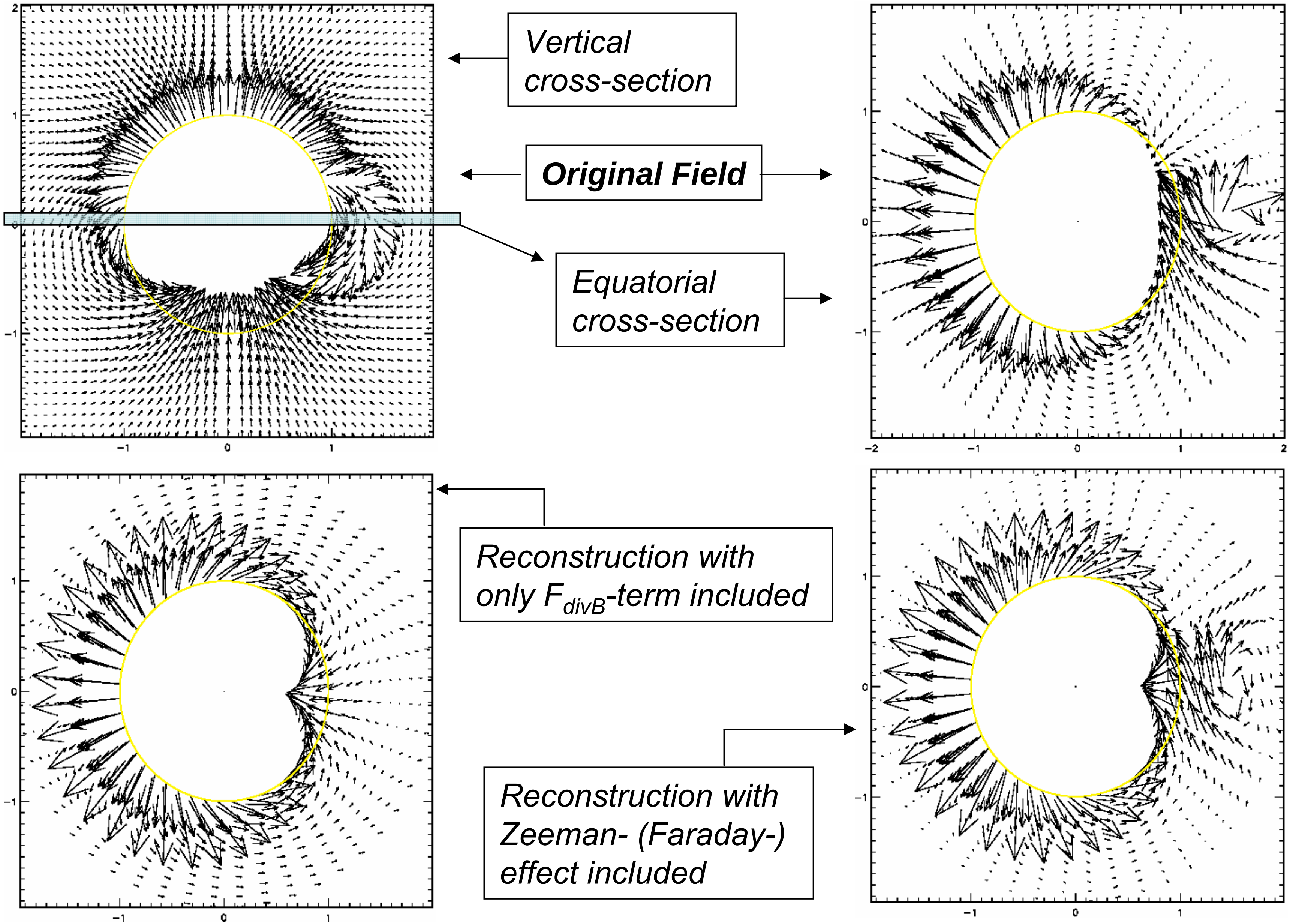

Reconstruction for Hanle-effect

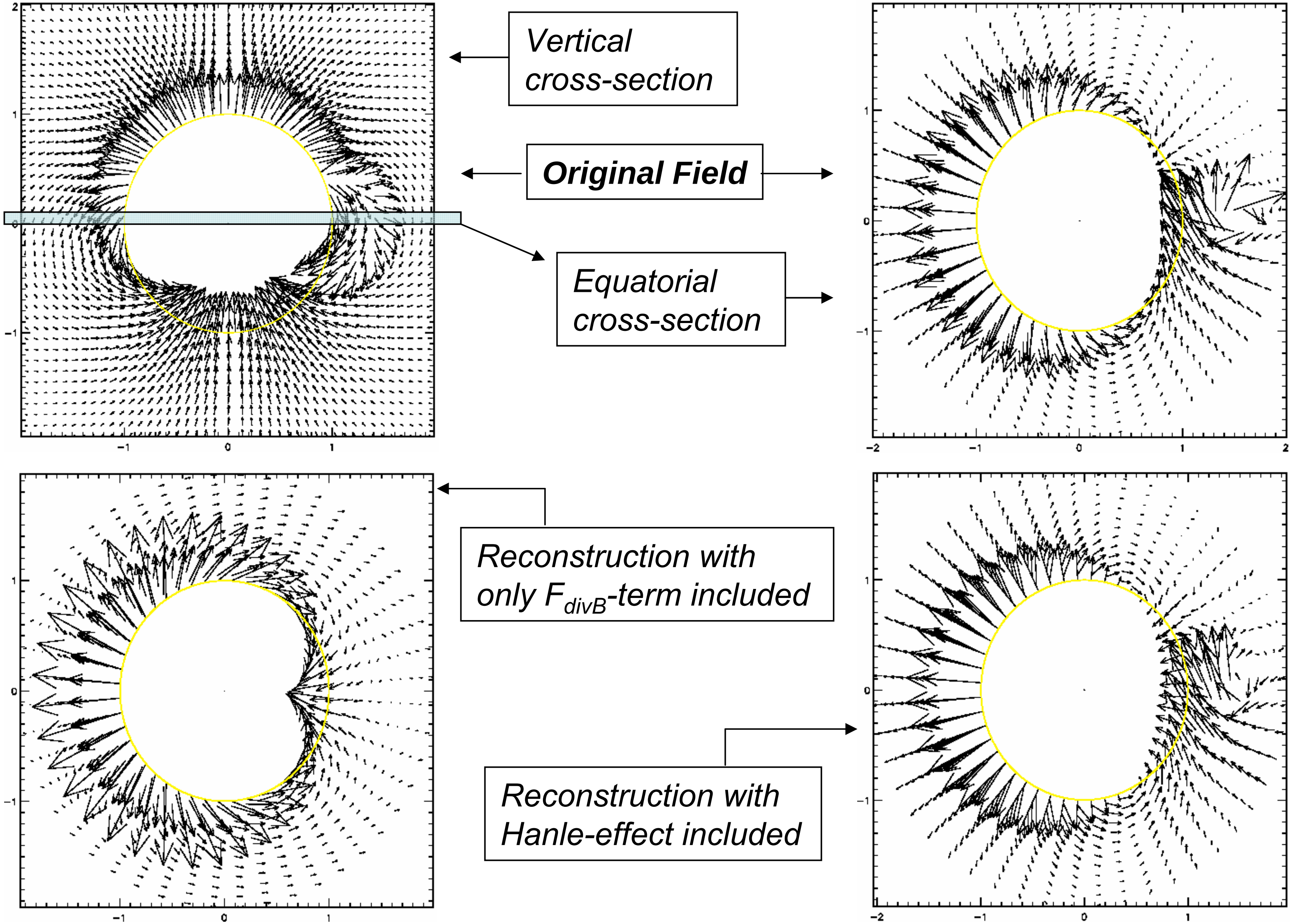

Reconstruction for Zeeman-, Hanle-effect

Zeeman-effect (solid bars) Hanle-effect (solid bars)

Dashed bars - potential field reconstruction

Angle between original vector and reconstructed one [°]

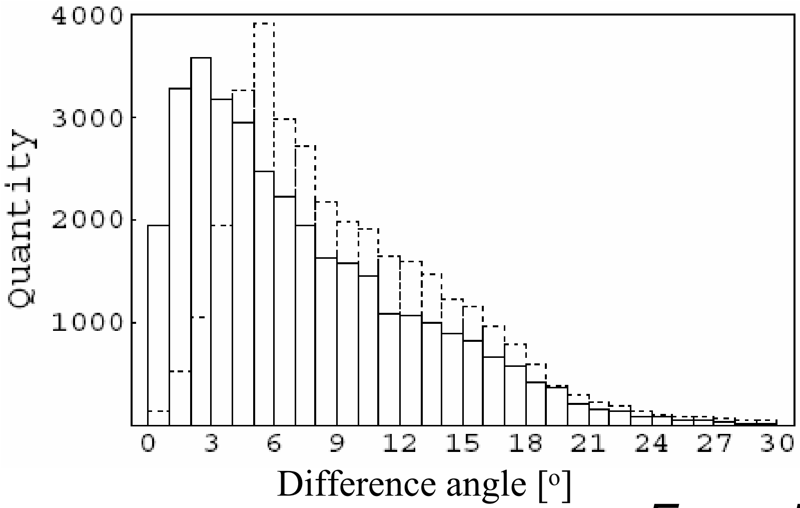

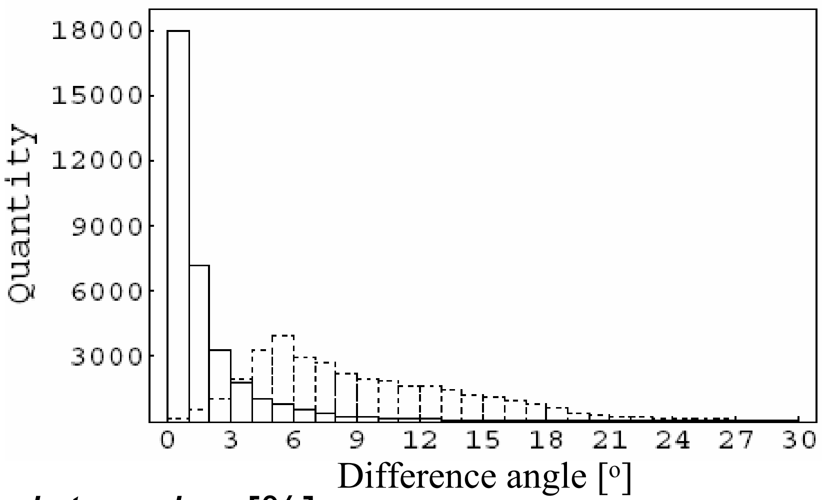

Errors in absolute value [%]

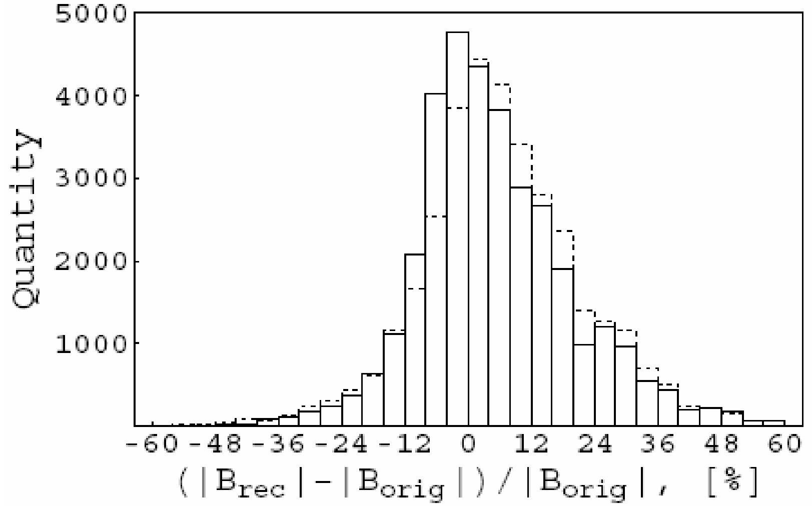

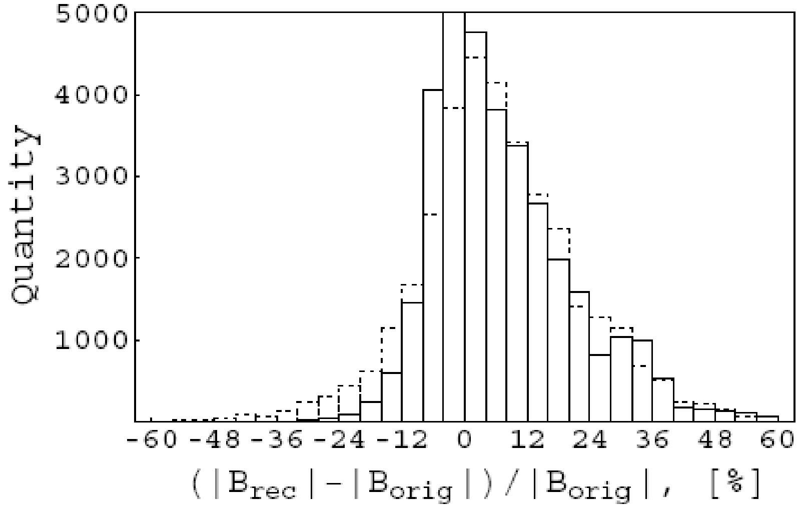

Reconstruction for Zeeman-, Hanle-effect

Zeeman-effect (solid bars)　　　　Hanle-effect (solid bars)

Dashed bars - potential field reconstruction

Angle between original vector and reconstructed one [°]

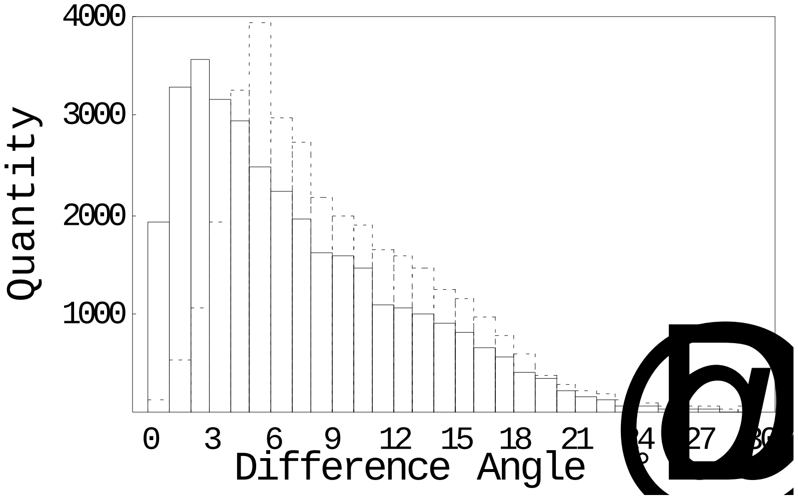

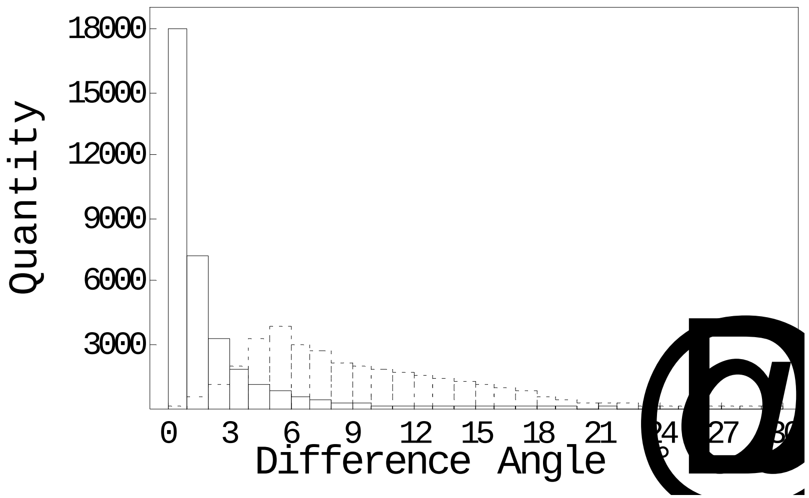

Errors in absolute value [%]

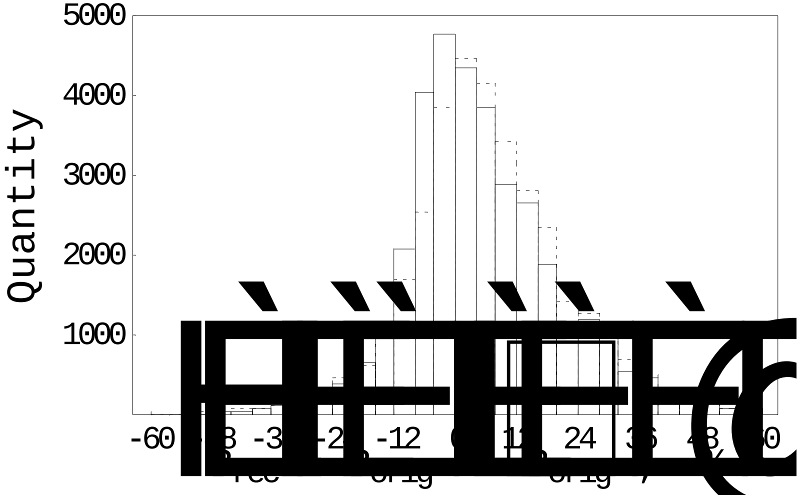

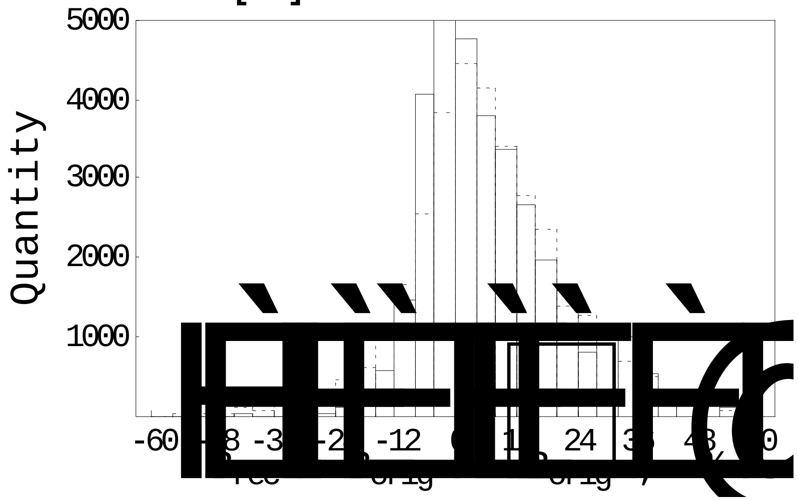

Conclusion

- Coronal Hanle and(or) Zeeman data **+** constraint $\nabla\cdot\boldsymbol{B}=0$ allows to reconstruct the non-potential component of the coronal magnetic field
- The tomographic inversions based on the Hanle effect and longitudinal Zeeman effect, have different precision for the different vector components of the field, depending on the configuration of the reconstructing field. Particularly, for the case of observation of a vortex-like field situated in the plane perpendicular to the rotation axis, the vortex is hardly seen in the reconstruction based on the Hanle effect, while the reconstruction based on the Zeeman effect gives saticfactory result for this field. The inversion based on the Hanle effect gives more precise result for the meridional component of the magnetic field than an inversion based on the Zeeman effect.

Conclusion

- Coronal Hanle and(or) Zeeman data **+** $\nabla \cdot \boldsymbol{B} = 0$ allows to reconstruct the non-potential component of the coronal magnetic field
- but ...

Outlook

- Different and more realistic coronal magnetic field configurations, e.g., the field above active regions or more realistic streamer-type field structures should be studied

- With the code we have developed, we can study with test calculations systematically how much noise is tolerable to achieve a certain precision of the solution.

- The influence of data gaps on the inversion result.

- Observations of the Faraday rotation of the linearly polarized radio signals traveling through the corona give information very similar to the longitudinal Zeeman effect. It would be interesting to study how useful these sparse measurements are for the reconstruction of the coronal field.

- In the code used in this thesis we neglected the alignment factor σ. A finite alignment factor will modify the numerical expressions for the inversion of the longitudinal Zeeman-effect data by about 30 % or less. For a quantitative application of our code to real data, a calculation of the alignment factor should be included.

- The inversion procedure presented here could be looked at as a first step towards a systematic line-of-sight inversion of all four Stokes components which would then yield not only the magnetic field but also the coronal density (mainly from the Stokes I component)

Outlook

- Influence of data gaps.
- Study systematically how much noise is tolerable to achieve a certain precision of the solution.
- Apply method to real data!
- Alternative data which can similarly be reconstructed:
  Faraday-rotation effect

  ⋮

- Our work is just a first step.
  Final goal: a systematic line-of-sight inversion of all four Stokes components.